(This is a sample cover image for this issue. The actual cover is not yet available at this time.)

Remote sensing of canopy light use efficiency in temperate and boreal forests of North America using MODIS imagery

Chaoyang Wu [a,b,*], Jing M. Chen [a], Ankur R. Desai [c], David Y. Hollinger [d], M. Altaf Arain [e], Hank A. Margolis [f], Christopher M. Gough [g], Ralf M. Staebler [h]

[a] Department of Geography and Program in Planning, University of Toronto, 100 St. George St., Toronto, ON, Canada M5S 3G3
[b] The State Key Laboratory of Remote Sensing Science, Institute of Remote Sensing Applications, Chinese Academy of Sciences, Beijing, 100101, China
[c] Department of Atmospheric & Oceanic Sciences, University of Wisconsin-Madison, Madison, WI, USA
[d] USDA Forest Service, Northern Research Station, 271 Mast Rd., Durham, NH, USA
[e] School of Geography and Earth Sciences, McMaster University, Hamilton, Ontario, Canada L8S 4K1
[f] Center d'Études de la Forêt, Faculté de Foresterie, de Géographie et de Géomatique, Université Laval, Québec, QC, Canada
[g] Department of Evolution, Ecology, and Organismal Biology, Ohio State University, Columbus, OH 43210, USA
[h] Science & Technology Branch, Environment Canada, Toronto, ON, Canada

ARTICLE INFO

ABSTRACT

Light use efficiency (LUE) is an important variable characterizing plant eco-physiological functions and refers to the efficiency at which absorbed solar radiation is converted into photosynthates. The estimation of LUE at regional to global scales would be a significant advantage for global carbon cycle research. Traditional methods for canopy level LUE determination require meteorological inputs which cannot be easily obtained by remote sensing. Here we propose a new algorithm that incorporates the enhanced vegetation index (EVI) and a modified form of land surface temperature (T_m) for the estimation of monthly forest LUE based on Moderate Resolution Imaging Spectroradiometer (MODIS) imagery. Results demonstrate that a model based on $EVI \times T_m$ parameterized from ten forest sites can provide reasonable estimates of monthly LUE for temperate and boreal forest ecosystems in North America with an R^2 of 0.51 ($p<0.001$) for the overall dataset. The regression coefficients (a, b) of the LUE–$EVI \times T_m$ correlation for these ten sites have been found to be closely correlated with the average EVI (EVI_ave, $R^2 = 0.68$, $p = 0.003$) and the minimum land surface temperature (LST_min, $R^2 = 0.81$, $p = 0.009$), providing a possible approach for model calibration. The calibrated model shows comparably good estimates of LUE for another ten independent forest ecosystems with an overall root mean square error (RMSE) of 0.055 g C per mol photosynthetically active radiation. These results are especially important for the evergreen species due to their limited variability in canopy greenness. The usefulness of this new LUE algorithm is further validated for the estimation of gross primary production (GPP) at these sites with an RMSE of 37.6 g C m^{-2} month^{-1} for all observations, which reflects a 28% improvement over the standard MODIS GPP products. These analyses should be helpful in the further development of ecosystem remote sensing methods and improving our understanding of the responses of various ecosystems to climate change.

© 2011 Elsevier Inc. All rights reserved.

1. Introduction

Forest ecosystems play an important role in global carbon sequestration (Beer et al., 2010; Zhao & Running, 2010). Annual global carbon uptake by vegetation, also referred to as gross primary production (GPP), is around 123 ± 8 petagrams of carbon per year (Beer et al., 2010). However, substantial variations in GPP are observed among different models and ecoregions, both at plant and stand levels, and these discrepancies illustrate the limits to our full understanding of the global carbon cycle.

Light use efficiency (LUE), defined as the amount of carbon fixed in photosynthesis per unit of absorbed solar radiation, is an important variable for the estimation of GPP from satellite inputs when using the Monteith equation (Monteith, 1972):

$$GPP = LUE \times APAR \tag{1}$$

where APAR is the absorbed photosynthetically active radiation calculated as the product of an absorbed fraction (f_{APAR}) and the amount of incident photosynthetically active radiation (PAR).

* Corresponding author at: Department of Geography and Program in Planning, University of Toronto, 100 St. George St., Toronto, ON, Canada M5S 3G3. Tel.: +1 647 524 0310.
E-mail address: hefery@163.com (C. Wu).

Typical methods for the simulation of LUE require prior specification of a maximum LUE (ε_0) for a specific land cover type and additional input of climate variables (e.g., temperature, water stress) representing canopy stresses that modulate this maximum LUE (Running et al., 2004). This method has been useful in productivity models, such as the Moderate Resolution Imaging Spectroradiometer (MODIS) GPP product (Running et al., 2004) and the Vegetation Photosynthesis Model (Xiao et al., 2004). However, the dependence on input climate variables and biome-scale maximum LUE can cause significant deviation from observed GPP (Heinsch et al., 2006; Mu et al., 2011; Zhao et al., 2006).

With ongoing improvements in our ability to remotely sense the land surface, there has been an increase in efforts to directly infer LUE using these observations. For example, the photochemical reflectance index (PRI), defined as a normalized difference index using reflectance at 531 and 570 nm, is suggested to have potential in tracking LUE both at the leaf scale based on ground spectral measurements (Filella et al., 2009; Gamon et al., 1997) and satellite observations (Drolet et al., 2005, 2008; Goerner et al., 2009; Hall et al., 2008; Hall et al., 2011; Hilker et al., 2009). However, PRI shows high sensitivity to various extraneous effects such as canopy structure and the view observer geometry, which prevents its use at landscape and global scales and requires the appropriate upscaling algorithms to account for structural differences in vegetation (Hilker et al., 2010). Hilker et al. (2008) shows that while isotropic PRI scattering is correlated to LUE variation, geometric scattering can be attributed to canopy level shading. Therefore, remote sensing of forest LUE from space would be achieved by measuring PRI as a function of shadow fraction using multi-angle observations (Hall et al., 2008), which is further confirmed by the relationship between spaceborne PRI and canopy shadow fractions (Hilker et al., 2009). A theoretical concept using a canopy reflectance model proposed by Hall et al. (2011) recently further validates that using PRI alone to predict canopy LUE is confounded by the shadow fraction viewed by the sensor.

A thorough analysis of PRI is shown in Garbulsky et al. (2011), indicating that calibration of the PRI-LUE relation across biomes and a careful attention to potentially confounding factors are both needed for future improvement. Apart from PRI, Inoue et al. (2008) demonstrate that a number of bands centered at the red edge and near-infrared ranges also have potential in deriving indicators of LUE for a wheat canopy. Correlations are reported between LUE and a number of vegetation indices, including the normalized difference vegetation index (NDVI, Rouse et al., 1974) and the enhance vegetation index (EVI, Huete et al., 2002) in crop (Wu et al., 2010, 2009) and peatland ecosystems (Schubert et al., 2010). However, the potential of a certain vegetation index as a proxy of LUE across biomes and the underlying mechanism are still unknown (Huemmrich et al., 2010; Zhang et al., 2009), probably due to a number of influencing factors, including temperature, soil moisture, vapor pressure deficit (VPD) and light quality (Coops et al., 2010).

Two specific aspects of known variations in LUE need to be considered for use in operational algorithms related to the use of vegetation indices. First, environmental effects of temperature and water stress considerably modify LUE and cannot be interpreted by a single vegetation index. These environmental controls likely limit the competency of productivity models that incorporate vegetation indices under drought conditions (Mu et al., 2011; Sims et al., 2008, 2006). A second uncertainty is the application of only a single vegetation index in evergreen biomes that show low dynamic ranges in greenness but potentially large variations in LUE (Garbulsky et al., 2008; Nakaji et al., 2008). Hence, environmental variables are potentially helpful in resolving these present limitations in remotely sensed LUE. A possible candidate among those climate variables is air temperature (T_a) because of its importance in influencing the magnitude and timing of plant growth (Chen et al., 2003), ecosystem respiration (Tang et al., 2008), LUE (Schwalm et al., 2006), and its correlation with other environmental variables, such as vapor pressure deficit

(VPD) and PAR (Sims et al., 2008). This potential has been demonstrated in previous studies, such as the MODIS GPP product which uses temperature and VPD to reduce LUE under unfavorable conditions (Running et al., 2004; Zhao et al., 2006). However, the dependence on the requirements of meteorological inputs at desired temporal and spatial scales generally limits its global application (Mu et al., 2011).

With the availability of global carbon flux data that can be used to calculate canopy level LUE for multiple ecosystems (Baldocchi, 2008), it is possible to validate and compare the candidate LUE models and their impacts on GPP for a broad array of forest types. Here we present a methodology for estimating monthly LUE using MODIS observations and compare simulated values against LUE derived from flux measurements obtained from multiple temperate and boreal forest sites within North America. MODIS-derived EVI and land surface temperature (LST) are examined for their potential in estimating monthly LUE across biomes. The objectives of this study are: (1) to analyze the potential of EVI in evaluating monthly LUE for both deciduous forests and evergreen forests, (2) to derive a new model that can provide better estimates of monthly LUE using the MODIS EVI and LST observations, and (3) to show the usefulness of the new LUE algorithm in the estimation of forest GPP. This effort could result in an improved algorithm for remote sensing of GPP and aid in understanding of terrestrial carbon cycle-climate feedbacks in forested ecosystems.

2. Materials and methods

2.1. Study sites

We focused on twenty forest sites in the North American flux networks, including twelve deciduous forests (DF) and eight evergreen forests (EF) (Fig. 1). Half of these sites, composed of five DF and five EF, were used to derive the LUE model and the remaining sites were used for validation. Detailed descriptions of these sites are shown in Table 1.

2.2. Flux and meteorological measurements

Flux data for the nine Canadian sites were downloaded from the Fluxnet-Canada Data Information System (http://www.fluxnet-canada.ca) while data for the other eleven AmeriFlux sites were acquired from http://public.ornl.gov/ameriflux/dataproducts.shtml. For all sites, months with modeled total GPP equal to or below zero or the mean T_a below zero were not used. To run models at a monthly temporal scale, sums of monthly precipitation and PAR were also generated.

For the Canadian sites, a standard procedure was used to estimate annual net ecosystem production (NEP) and to partition NEP into components of GPP and ecosystem respiration (R_e) from gap-filled half-hourly measurements (Barr et al., 2004). Empirical regressions of nighttime NEE to temperature and daytime GPP to PAR were used to estimate GPP and R_e and fill gaps as discussed in more detail in Barr et al. (2004).

For the AmeriFlux sites, level-4 monthly products were used for the monthly GPP, air temperature (T_a) and radiation measurements. These data were gap-filled with the Artificial Neural Network (ANN) method (Papale & Valentini, 2003) and/or the Marginal Distribution Sampling (MDS) method (Reichstein et al., 2005). Flags with information regarding the quality of the original and gap-filled data were also added.

Desai et al. (2008) show that while partitioning methods can cause GPP or R_e estimates to vary widely (~20%), using consistent methodology across sites allows for robust characterization of differences in GPP and R_e across space and time. This is because flux tower NEE generally constrains GPP and R_e to a range of magnitudes that do not strongly depend on partitioning technique, but care must be taken in this process, as discussed in more detail in Desai et al. (2008).
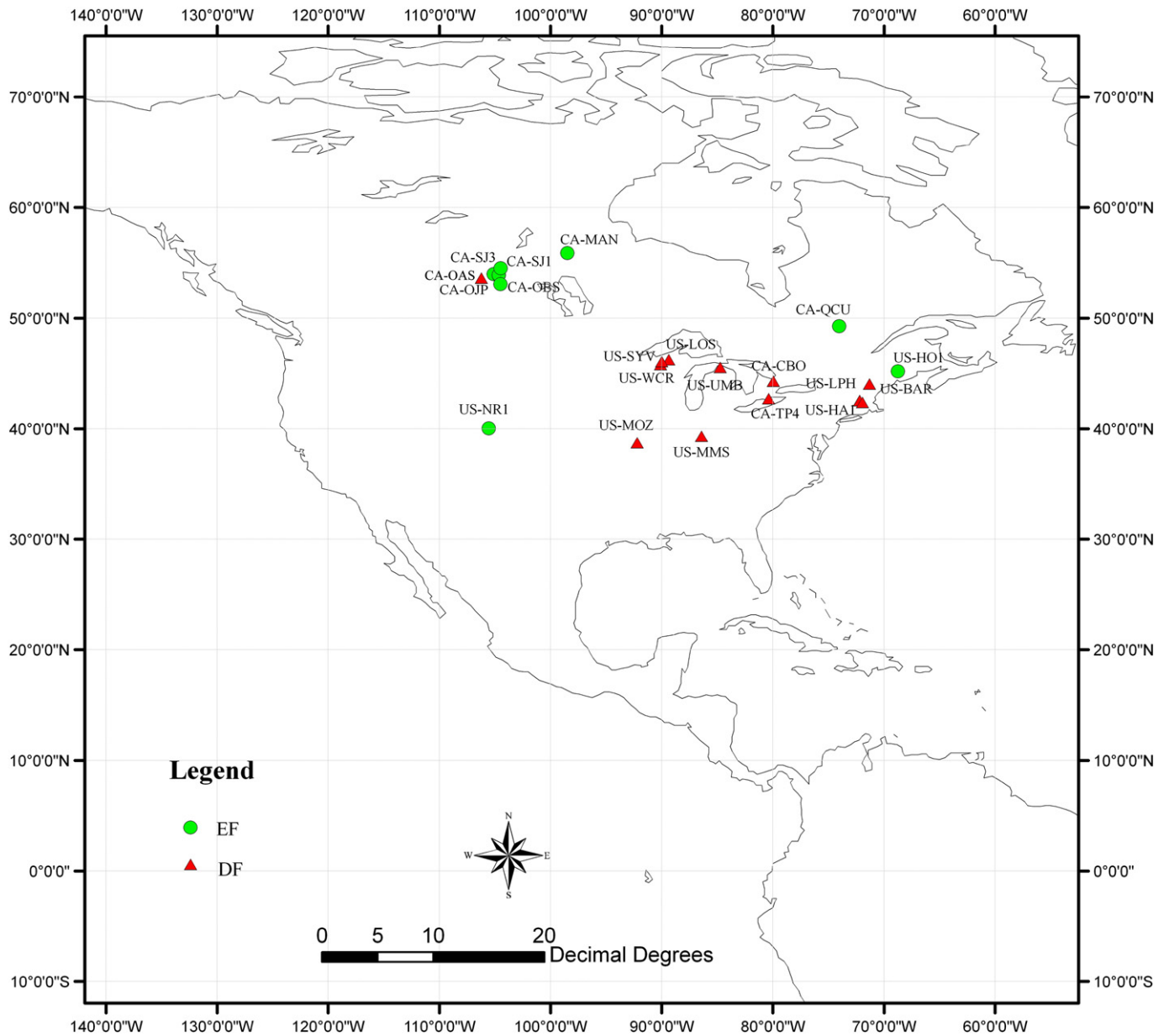
Fig. 1. Spatial distribution of the twenty sites in this study, DF and EF represent deciduous forest and evergreen forest sites, respectively.

2.3. MODIS products

Three derived MODIS land surface products were used in this study. These data for each site were acquired at the Oak Ridge National Laboratory's Distributed Active Archive Center (DAAC) website (http://www.modis.ornl.gov/modis/index.cfm). The first is the 16-day Terra MODIS vegetation index product (MOD13Q1, 250 m, collection 5) that provides both NDVI and EVI computed from atmospherically corrected bi-directional surface reflectance which have been masked for water, clouds, heavy aerosols, and cloud shadows. For each site, both NDVI and EVI were extracted from 3×3 MODIS pixels centered on the flux tower similar to the approach used by Sims et al. (2008). The 3×3 MODIS pixels method was also checked at each site with respect to both footprints (~1 km) and land cover (Chen et al., 2011).

The second product is the MODIS GPP product (MOD17A2, 1 km, collection 5.1), which is included in this study for model comparison. MODIS GPP is driven by daily MODIS landcover, f_{APAR}/LAI and

interpolated surface meteorology at 1 km for the global vegetated land surface (Zhao et al., 2006). This product is calculated using LUE as:

$$GPP = \varepsilon_{max} \times m(T_{min}) \times m(VPD) \times FPAR \times SWrad \times 0.45 \quad (2)$$

where ε_{max} is the maximum LUE obtained from lookup tables on the basis of vegetation type. The scalers m(Tmin) and m(VPD) reduce ε_{max} under unfavorable conditions of low temperature and high VPD. Tmin, VPD and SWrad are obtained from large spatial-scale meteorological data sets that are available from the NASA Global Modeling and Assimilation Office (GMAO) (http://gmao.gsfc.nasa.gov/).

The most recent update to the 8-day GPP products also corrects previous issues arising from cloud contamination (Zhao et al., 2006). Since it is not straightforward to determine which pixel the tower footprint primarily falls in, we have applied both the central and mean values of 3×3 pixels. Preliminary results indicated that the latter provided better correlation with GPP from flux measurements, and

Table 1
Description of flux sites in this study (DF and EF represent deciduous and evergreen forests, respectively).

Code	Site name	Land cover	Latitude	Longitude	Data range	References	Note
US-MMS	Morgan Monroe State Forest	DF	39.3231	−86.4131	2002–2006	Dragoni et al. (2007)	Calibration sites
US-HA1	Harvard Forest	DF	42.5378	−72.1715	2003–2006	Urbanski et al. (2007)	
US-UMB	Univ. of Mich. Biological Station	DF	45.5598	−84.7138	2002–2006	Curtis et al. (2002)	
US-WCR	Willow Creek	DF	45.8059	−90.0799	2002–2006	Cook et al. (2004)	
US-SYV	Sylvania Wilderness	DF	46.2420	−89.3477	2002–2006	Desai et al. (2005)	
US-NR1	Niwot Ridge	EF	40.0329	−105.5460	2004–2007	Monson et al. (2005)	
US-HO1	Main Howland Forest	EF	45.2041	−68.7402	2002–2004	Hollinger et al. (2004)	
CA-OJP	Old Jack Pine	EF	53.9163	−104.6920	2003–2007	Coursolle et al. (2006)	
CA-OBS	Southern Old Black Spruce	EF	53.9871	−105.1177	2003–2007	Barr et al. (2004)	
CA-QCU	Harvested Black Spruce/Jack Pine	EF	49.2671	−74.0365	2005–2009	Giasson et al. (2006)	
US-BAR	Bartlett Experimental Forest	DF	44.0646	−71.2881	2004–2006	Jenkins et al. (2007)	Validation sites
US-LPH	Little Prospect Hill	DF	42.5419	−72.1850	2002–2004	Hadley et al. (2008)	
US-LOS	Lost Creek	DF	46.0827	−89.9792	2003, 2005	Denning et al. (2003)	
US-MOZ	Missouri Ozark	DF	38.7441	−92.2000	2006–2007	Gu et al. (2007)	
CA-OAS	Old Aspen	DF	53.6288	−106.1977	2004–2008	Barr et al. (2004)	
CA-CBO	Borden Mixedwood	DF	44.3185	−79.9342	2004–2006	Teklemariam et al. (2009)	
CA-TP4	Turkey Point White Pine 1939	DF	42.7097	−80.3574	2004–2007	Arain et al. (2006)	
CA-SJ3	Jack Pine 1975	EF	53.8758	−104.6452	2004–2007	Amiro et al. (2006)	
CA-SJ1	Jack Pine 1994	EF	53.9084	−104.6559	2003–2005	Amiro et al. (2006)	
CA-MAN	Northern Old Black Spruce	EF	55.8800	−98.4810	2004–2007	Dunn et al. (2007)	

therefore we subsequently relied on that value to estimate MODIS-derived tower GPP.

We also extracted MODIS 8-day Land Surface Temperature (LST) and Emissivity product (MOD11A2, 1 km) derived by applying the generalized split-window algorithm. In the split-window algorithm, emissivity in bands 31 and 32 are estimated from land cover types, and atmospheric column water vapor and lower boundary air surface temperature are separated into tractable sub-ranges for optimal retrieval (Wan, 2008).

2.4. Calculation of LUE

One important step in calculating canopy level LUE is the determination of f_{APAR}, which is a parameter indicating the green biomass within a canopy that absorbs radiation. Given the well established correlation between NDVI and f_{APAR} (Fensholt et al., 2004; Huemmrich et al., 2010; Viña & Gitelson, 2005), we used the empirical relationship validated for many AmeriFlux ecosystems (Sims et al., 2006),

$$f_{APAR} = 1.24 NDVI - 0.168 \tag{3}$$

where the NDVI is extracted from the MODIS vegetation index product.

We use these coefficients because they have been validated previously by Sims et al. (2006) in five of our study sites (US-NR1, US-HO1, US-HA1, US-MMS and CA-MAN), which give more confidence in the use of this relationship.

Two other methods of f_{APAR} calculation were adopted for two specific sites, providing an opportunity to compare various methods in LUE calculation. In site US-WCR, radiation at different heights was measured and therefore the f_{APAR} can be directly calculated by:

$$f_{APAR} = \frac{PAR_{30} - PAR_2}{PAR_{30}} \tag{4}$$

where PAR_{30} and PAR_2 represent for the PAR at 30 m and 2 m, which span above canopy and below canopy, respectively. The calculation of f_{APAR} has been validated in this site because the relative difference in above canopy and bottom of canopy PAR is a good measure of true APAR (Cook et al., 2008, 2009).

For site US-MMS, where temporal in situ LAI data were available, the f_{APAR} was calculated using the mean in situ LAI, light extinction coefficient (k = 0.5) and the following equation (Xiao et al., 2004):

$$f_{APAR} = 0.95 \left(1 - e^{-kLAI}\right) \tag{5}$$

After the calculation of f_{APAR}, the LUE was determined as,

$$LUE = \frac{GPP}{f_{APAR} \times PAR} \tag{6}$$

2.5. Structure of this analysis

To give a clear description of the structure of our analysis, we provided a section about the methods and procedures in the deriving and validation of our model. We first explored the potential of the EVI as an indicator of canopy LUE across all sites as well as the factors that can influence this correlation. Then, we used half of all sites, five DF and five EF sites, respectively, to derive a new model that can estimate the canopy LUE with a combination of MODIS EVI and LST. The calibration process was also conducted for these ten sites in order to determine the coefficients of the predicting model. The calibrated model was then validated for the estimation of LUE in the remaining ten independent sites to show the robustness of our algorithm. Finally, we further applied this new LUE algorithm for the estimation of GPP and compared with the standard MODIS GPP for all sites. Some in-depth discussions on both the perspectives and limitations of our model were also included.

3. Results

3.1. Relationship between LUE and EVI

The relationship between all tower-derived monthly LUE and remotely sensed EVI reveals a relationship with a coefficient of determination (R^2) equal to 0.46 (Fig. 2a) with evident differences among forest functional types. An R^2 of 0.62 was found for deciduous forest (DF) sites, suggesting that EVI can better simulate the dynamics of LUE for ecosystems with wider dynamical ranges in EVI. For example, EVI values for DF sites generally fluctuated between 0.15 and 0.75 with a mean standard deviation (sd) of among months around 0.15. The LUE in DF sites was closely related to phenological
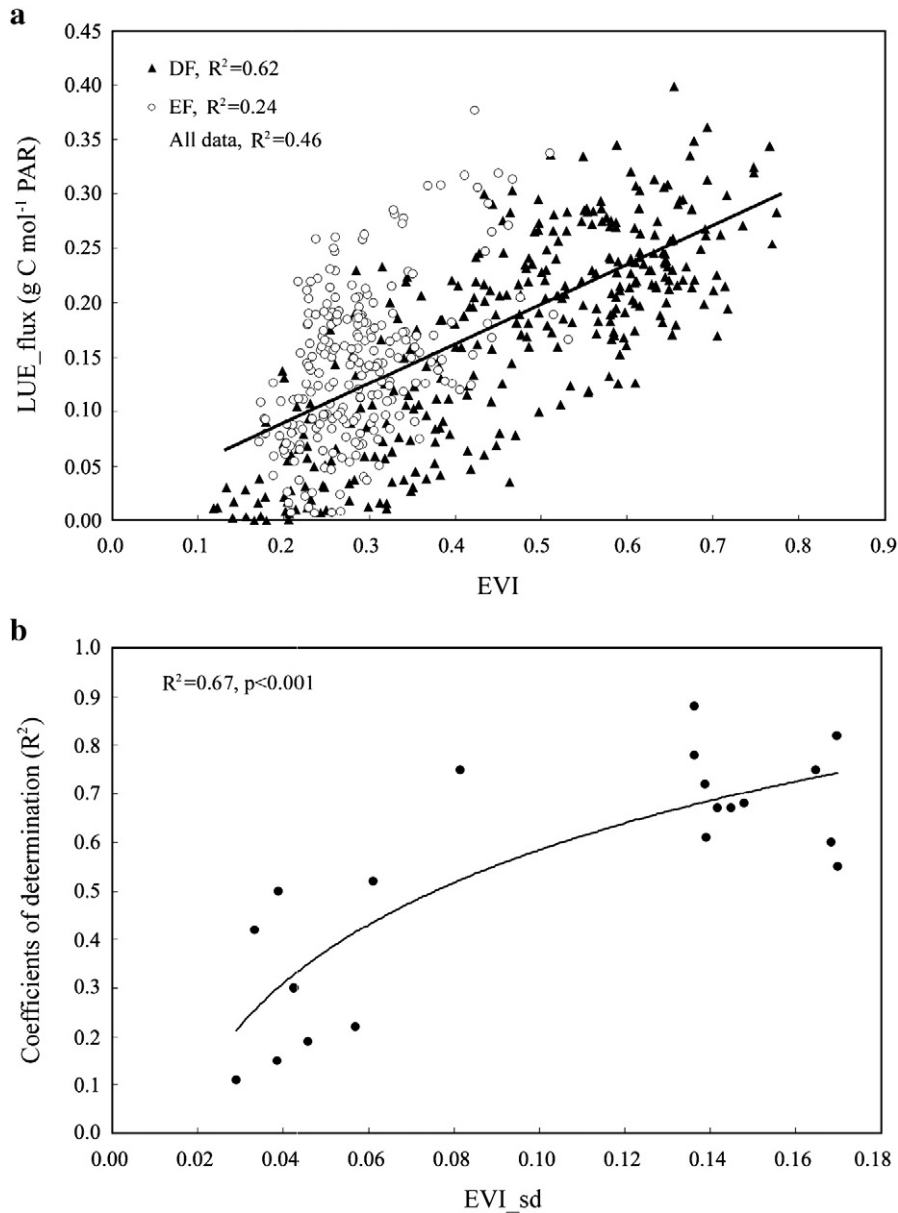
Fig. 2. (a) Relationship between the flux-measured LUE and the MODIS-derived EVI for data in this study, DF and EF represent deciduous forest and evergreen forest, respectively. The regression line for the overall data is $y = 0.36x + 0.02$ ($R^2 = 0.46$, $p < 0.001$). (b) Relationship between R^2 of EVI–LUE correlation and the standard deviation in EVI (EVI_sd) for each site during the experimental period, the regression line is $y = 0.30 \ln(x) + 1.28$ ($R^2 = 0.67$, $p < 0.001$).

characteristics, which tend to track LUE, and thus EVI is a good approximation of LUE.

However, for EF sites, the EVI values fall in the narrow range of 0.15–0.50 with limited monthly variability (sd = 0.05). Not surprisingly, we find the LUE–EVI relationship had a much lower coefficient of determination ($R^2 = 0.24$). A further analysis (Fig. 2b) reveals a positive correlation ($R^2 = 0.67$, p = 0.001) between the R^2 of EVI-LUE relationship and the sd of EVI (EVI_sd) for each site during the experimental period. These findings suggest that EVI is not a reliable indicator of LUE for biomes with limited seasonal variability in greenness, and that other variables should be incorporated to characterize LUE in these evergreen biomes.

3.2. Relationship between LUE and temperature

In the following sections, only the calibration sites were used. The relationship between tower-observed monthly air temperature and LUE was similar in strength to that of LUE and EVI ($R^2 = 0.43$, Fig. 3a). When the relationship was partitioned by functional types, T_a better explained the variances in monthly LUE for DF sites than for EF sites. EVI has a stronger mechanistic link to LUE, but clearly the relationship to T_a also predicts seasonality. For the DF sites, T_a is a simple and consistent proxy for canopy phenological processes that regulate seasonal changes in LUE. Thus, both EVI and T_a are found to be correlated with canopy LUE. However, for EF sites, little variation is expected in canopy greenness and the T_a mainly acts as a limiting factor to canopy physiological functioning, including GPP. In this case, monthly LUE is better correlated with T_a ($R^2 = 0.34$) than to the EVI ($R^2 = 0.24$).

Since canopy air temperature cannot be directly observed by remote sensing, we compared observations of T_a to the MODIS LST product as an important step for scaling the algorithm up for global remote sensing. We find that MODIS LST can be a non-linear function of T_a with coefficients of determination R^2 of 0.78 for the overall data-set, without radiometric to air temperature correction considered (Fig. 3b). No difference was observed between the two plant
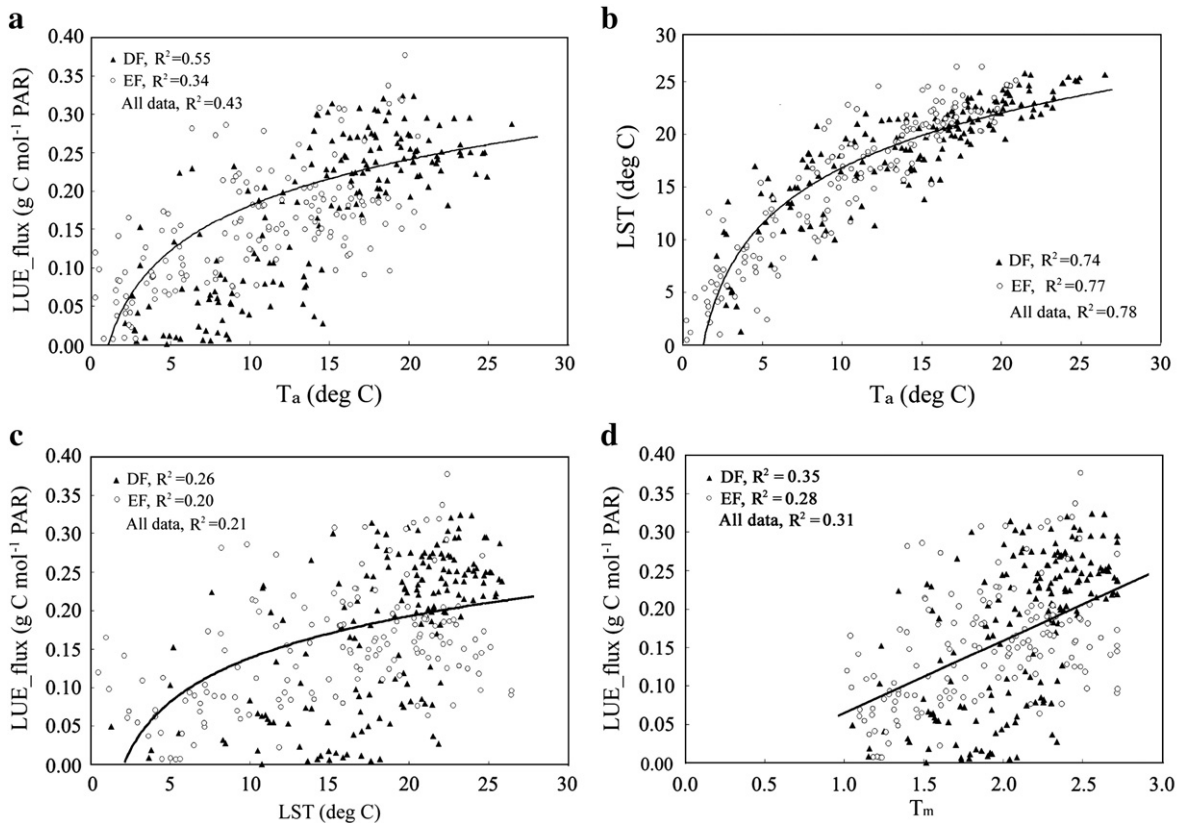
Fig. 3. Relationship between the flux-measured LUE (LUE_flux) and temperature at the calibration sites, DF and EF represent deciduous forests and evergreen forests, respectively. (a) Correlation between LUE_flux and T_a, the regression line for overall data is $y = 0.07\ln(x) - 0.01$ ($R^2 = 0.43$, $p < 0.001$); (b) Correlation between MODIS LST and T_a from flux measurements, the regression line for overall data is $y = 7.19\ln(x) + 0.24$ ($R^2 = 0.78$, $p < 0.001$); (c) Correlation between LUE_flux and LST, the regression line for overall data is $y = 0.07\ln(x) - 0.03$ ($R^2 = 0.21$, $p < 0.001$); (d) Correlation between LUE_flux and the modified LST (T_m), the regression line for overall data is $y = 0.11x - 0.05$ ($R^2 = 0.31$, $p < 0.001$).

functional types as comparable correlations were acquired with R^2 of 0.74 and 0.78 for DF and EF sites, respectively. However, the MODIS LST tends to overestimate T_a below 25 °C. The 1 km LST signal measures a combination of the radiant temperature of the land surface and the intervening atmosphere (Goetz et al., 2000). The role of cloud contamination may be the largest uncertainty in these data because of the inherent limitation of the thermal infrared remote sensing, including the failure to remove cloud-contaminated LST, as well as the different degrees of influence of cloud contamination between estimation of LST and emissivity (Wan, 2008).

A problem with using temperature as an indicator of LUE (Fig. 3c) is the decreasing sensitivity of LUE at high temperature values. Consequently, we find logarithmic regressions give the best fit between LUE and T_a or LST. This suggests a declining response to temperature for LUE, probably because T_a is only a good predictor when phenology is dynamic. Once temperatures reach high values during the growing season, LUE will show less sensitivity to T_a since phenology has stabilized. Therefore, here we provide a modified form of LST (T_m) as below:

$$T_{m,i} = \exp(LST_i / LST_{max}) \tag{7}$$

where LST_i is the mean ith month temperature and LST_{max} is the maximum monthly temperature of the site for experimental years. The exponential transform can improve the LUE sensitivity at high temperatures. We suspect that incorporating a multi-year maximum temperature may be potentially helpful for capturing the effects of both seasonal and interannual variations of temperature on LUE.

The usefulness of T_m is shown in Fig. 3d where the log transform allows us to produce a linear correlation between LUE and T_m with coefficient of determination R^2 of 0.31 for the overall data. For the

EF sites, no evident effect was observed with the T_m, probably owing to the low temperature ranges (mean $T_a = 15.3$ °C for all EF sites). However, in contrast, we find R^2 of 0.35 for the DF sites which have higher monthly temperatures (mean $T_a = 18.6$ °C for all DF sites) and these results highlight the suitability of T_m instead of LST for LUE remote sensing in DF.

3.3. Estimating LUE using $EVI \times T_m$

Given the relationships between LUE and both EVI and T_m, especially in DF, we developed a new model that incorporates both EVI and T_m, $EVI \times T_m$, to estimate monthly LUE (Fig. 4). A stronger
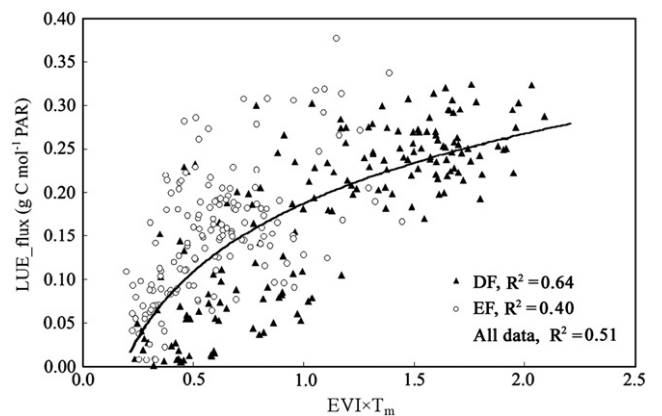

Fig. 4. Relationship between the flux-measured LUE and $EVI \times T_m$ for data in this study, DF and EF represent deciduous forests and evergreen forests, respectively. The regression line for the overall data is $y = 0.11\ln(x) + 0.20$ ($R^2 = 0.51$, $p < 0.001$).

relationship ($R^2 = 0.51$, p<0.001) is found between LUE and $EVI \times T_m$ than for either variable alone. Improvements are shown for both DF ($R^2 = 0.64$) and EF ($R^2 = 0.40$) sites with this new model, as indicated by higher coefficients of determination when compared with either EVI or T_m.

The new model is able to replicate the temporal evolution and magnitude of LUE, but with a range of performance among sites (Table 2). For the DF sites, the highest coefficients R^2 of 0.85 are observed for US-HA1 and the lowest precision is acquired in US-SYV with R^2 of 0.58. The other three DF sites (US-MMS, US-UMB and US-WCR) generally show a similar range of R^2 between 0.61 and 0.71. For EF sites, the model generally gives moderate accuracy with R^2 ranges from 0.51 for US-NR1 to the largest of 0.64 for CA-QCU. These results indicate that the $EVI \times T_m$ can be a potential candidate of LUE for different plant functional types, improving on existing models that only use EVI to predict LUE.

With results for these ten sites, the monthly LUE can be estimated as:

$$LUE = a \ln(EVI \times T_m) + b \qquad (8)$$

Significant correlation is observed between the coefficient a and the average EVI (EVI_ave) of the experimental period with an R^2 equals to 0.68 (p = 0.003, Fig. 5a). The coefficient b, meanwhile, has been found to be correlated with the minimum monthly LST (LST_min, $R^2 = 0.81$, p = 0.009, Fig. 5b). Therefore, the coefficients for the calibrated LUE algorithm can be written as:

$$a = 0.21 EVI\_ave + 0.04$$
$$b = -0.04 \ln(LST\_min) + 0.25 \qquad (9)$$

Fig. 6 shows the comparison between the modeled LUE and measured LUE for each site. The use of this model for estimating LUE in each site shows good agreement, with the largest root mean square error (RMSE) of 0.068 g C mol^{-1} PAR in US-UMB to the lowest of 0.026 g C mol^{-1} PAR in US-NR1.

We further used the calibrated model to predict LUE for the ten validation sites (Fig. 7). Good estimates of LUE are observed for both the DF and EF sites with respective R^2 of 0.68 and 0.48 and an overall monthly RMSE of 0.055 g C mol^{-1} PAR. The proposed model gives large improvements for the EF sites indicating the new algorithm is still suitable for the evergreen forests, even with the previous caveats raised about weaker relationships among EVI, T_m, and LUE.

3.4. Evaluation of $EVI \times T_m$ model performance

As the model is derived by incorporation of both effects of greenness and temperature on LUE, it is useful to investigate model performance as a function of variables indicating the regional and biophysical properties of a site. As shown in Fig. 8a, the model performance, indicated by the R^2 of LUE–$EVI \times T_m$ relationship, is related to the maximum EVI

Table 2
Correlation between LUE and $EVI \times T_m$ for each calibration sites.

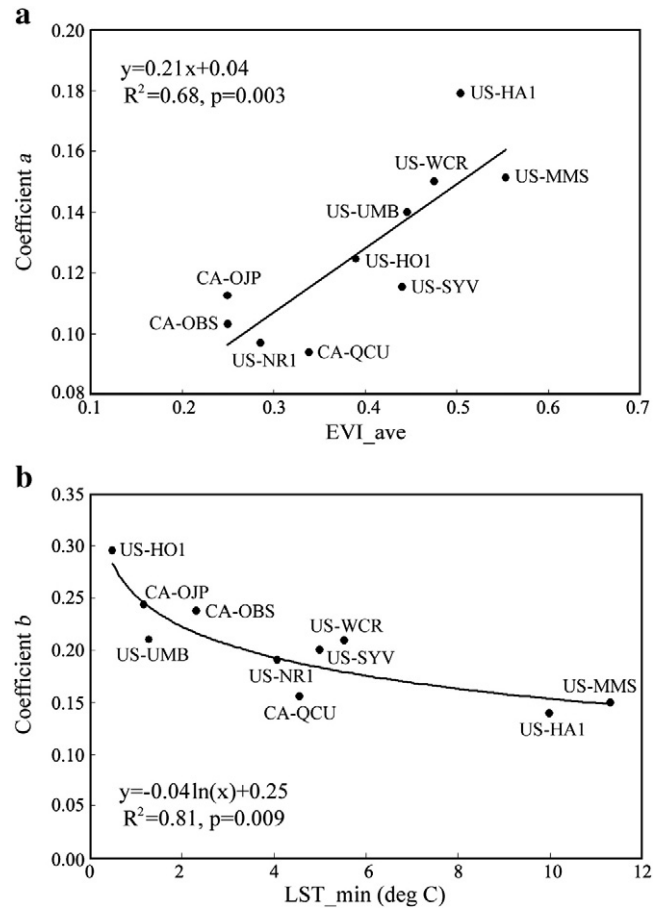| Site code	Coefficient a	Coefficient b	R^2	p value
US-MMS	0.1512	0.1498	0.61	<0.001
US-HA1	0.1791	0.1391	0.85	<0.001
US-UMB	0.1399	0.2101	0.65	<0.001
US-WCR	0.1500	0.2089	0.71	<0.001
US-SYV	0.1154	0.2003	0.58	<0.001
US-NR1	0.0971	0.1908	0.51	<0.001
US-HO1	0.1245	0.2954	0.51	<0.001
CA-OJP	0.1125	0.2437	0.51	<0.001
CA-OBS	0.1031	0.2376	0.52	<0.001
CA-QCU	0.0938	0.1555	0.64	<0.001

Fig. 5. The relationships between the regression coefficients of LUE–$EVI \times T_m$ and (a) average EVI (EVI_ave), (b) the minimum monthly LST (LST_min) for each calibration site.

(EVI_max, $R^2 = 0.56$, p<0.001) which implies that the proposed model will give better estimates of monthly LUE for ecosystems that have high EVI values. Interestingly, mean monthly precipitation (Precip_ave) also shows a positive impact on the estimation of LUE using $EVI \times T_m$ (Fig. 8b, $R^2 = 0.50$, p<0.001, US-LPH, CA-SJ1, CA-SJ3 and CA-MAN were excluded due to unavailable of precipitation data).

4. Discussions

4.1. Application of this LUE algorithm to estimate GPP

When the new model was applied to estimate GPP, we also observed a better performance than the standard MODIS GPP products. An R^2 of 0.73 (p<0.001) and an overall RMSE of 52.7 g C m^{-2} month^{-1} are obtained between the flux-measured GPP and the MODIS GPP products for all sites (Fig. 9a). Similar to our findings, MODIS GPP also shows better suitability for DF sites ($R^2 = 0.71$, RMSE = 60.7 g C m^{-2} month^{-1}) than for EF sites ($R^2 = 0.67$, RMSE = 35.7 g C m^{-2} month^{-1}). For all observations, there is a clear pattern for MODIS GPP to be higher than flux GPP at the low end of the range while lower than flux GPP at the upper end of the GPP range. Similar results were also reported in previous studies both at plots and continental scales (Sjöström et al., 2011; Wu et al., 2011; Xiao et al., 2010). We suggest that the improper characterization of shaded leaves in dense canopies is the main reason for the underestimation of high GPP. This hypothesis is supported by recent study of Cheng et al. (2009) which reports the correlation between flux-measured LUE and the reflectance difference between shaded and sunlit leaves in a canopy. These observations also agree with the improvements on reflectance simulations from radiative transfer models incorporation of a lower canopy layer comprised of
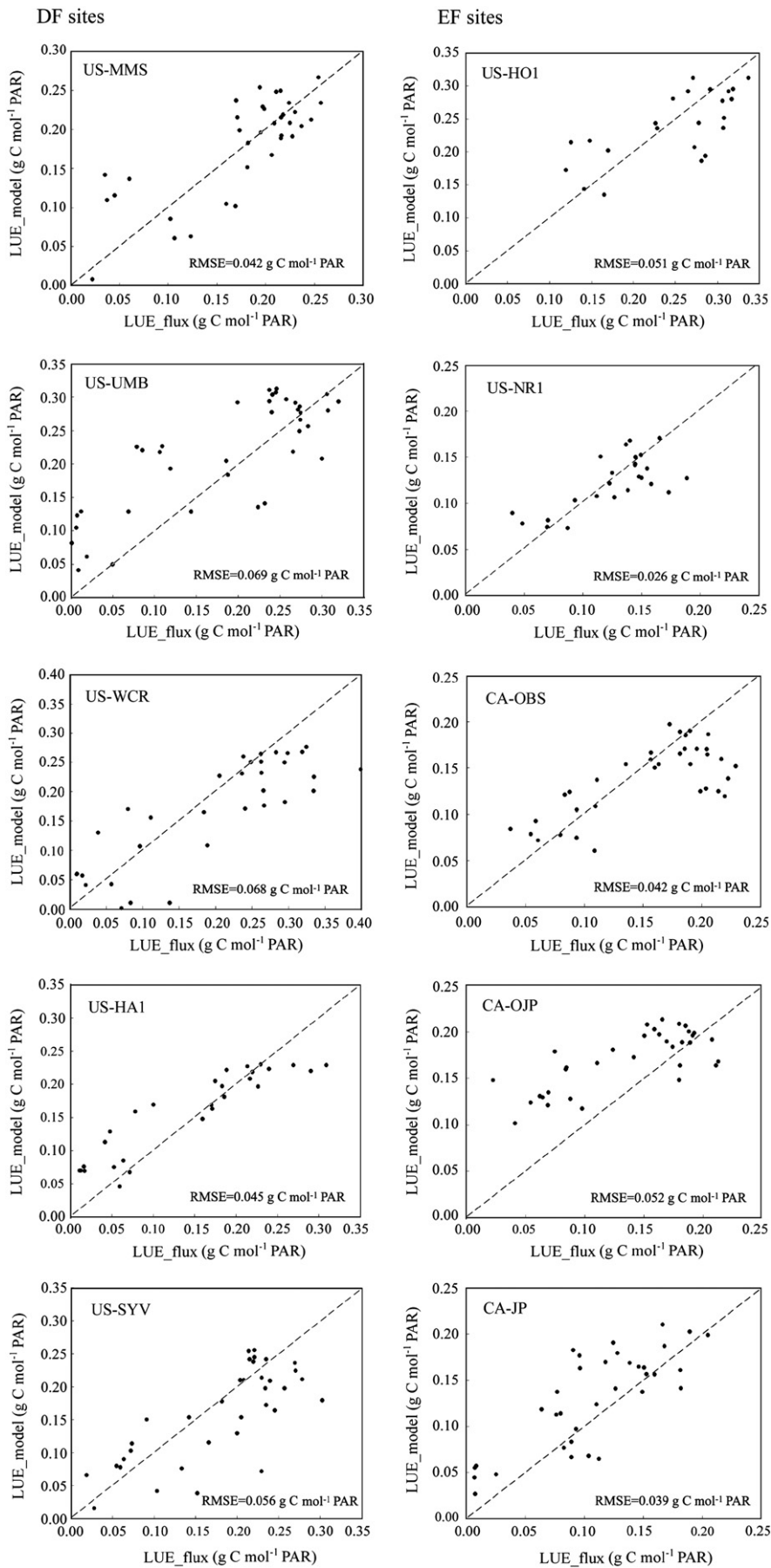
Fig. 6. Relationship between the flux-measured LUE and model outputs for each modeling site in this study, DF and EF represent deciduous forests and evergreen forests, respectively.
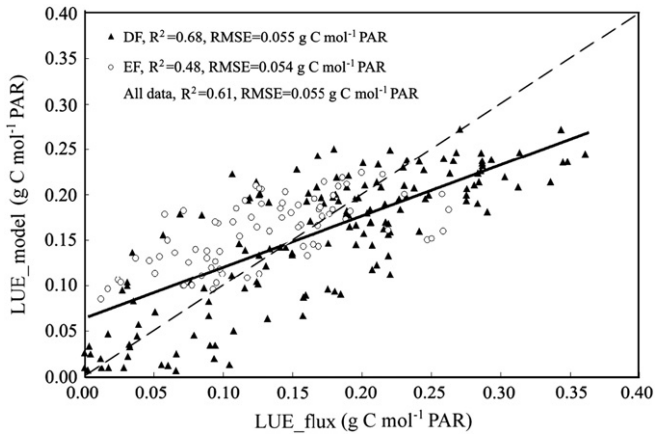
Fig. 7. Relationship between the flux-measured LUE and modeled LUE for the validation sites, DF and EF represent deciduous forests and evergreen forests, respectively. The regression for the overall dataset is $y = 0.570x + 0.065$ ($R^2 = 0.61$, $p < 0.001$).

shaded leaves beneath the upper sunlit leaf layer (Cheng et al., 2010). To balance this limitation, overestimations are observed for low GPP ranges as regression model commonly gives the average situation of variables. A direct impact of these misinterpretations is the limited potential in characterizing LUE that a relatively low correlation between MODIS-derived LUE and flux measurements that was observed with our dataset ($R^2 = 0.32$, Fig. 9b).

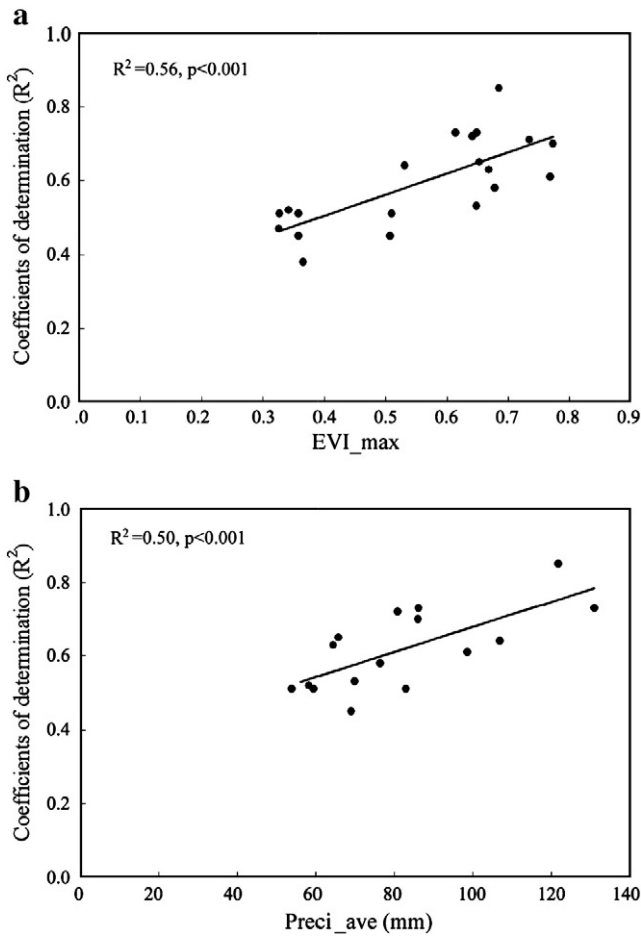When the new LUE using our method is introduced, large improvements are observed for both the overall dataset

Fig. 8. Relationship between the determination coefficients R^2 of LUE–EVI$\times$T$_m$ and the maximum EVI (EVI_max), average precipitation (Preci_ave) for all sites.
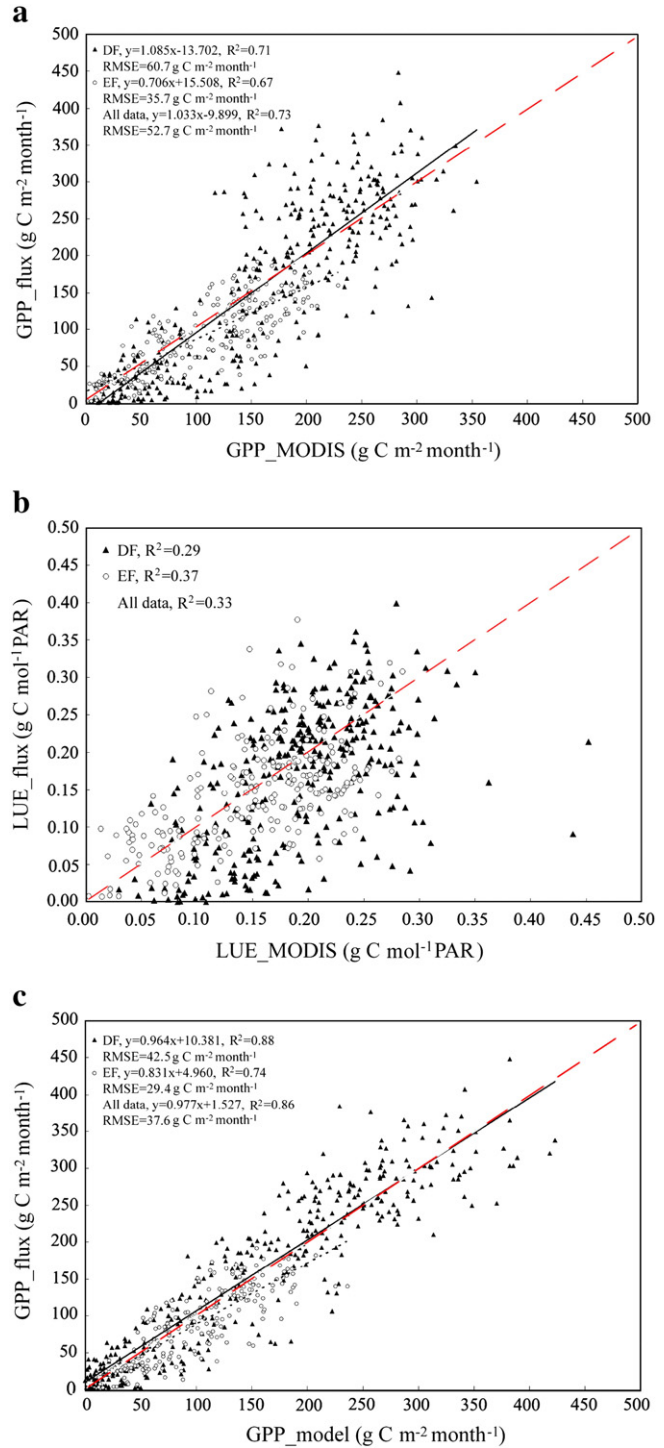

Fig. 9. Comparison between the (a) flux-measured GPP and MODIS GPP, (b) flux-measured LUE and the GPP LUE, (c) the flux-measured GPP and GPP using the proposed LUE algorithm (solid and dash lines represent regressions DF and EF, respectively, the red indicates the 1:1 line). For interpretation of the references to color in this figure legend, the reader is referred to the web version of this article.

($R^2 = 0.86$, RMSE $= 37.6$ g C m^{-2} month^{-1}), DF sites ($R^2 = 0.88$, RMSE $= 42.5$ g C m^{-2} month^{-1}), and EF sites ($R^2 = 0.74$, RMSE $= 29.4$ g C m^{-2} month^{-1}) (Fig. 9c). No significant bias exists for these observations and the issue of overestimation at high GPP values is largely reduced, indicating the high sensitivity of the model for regional application with a wider dynamical range in GPP. This application of GPP estimation in multi-ecoregions also indicates that the new LUE algorithm can be of potential use for

carbon cycle analysis in various ecosystems that have diverse canopy structures and climate characteristics. Moreover, a significant advantage of this algorithm is the lack of a requirement for interpolated meteorological inputs, which have been shown to add significant bias to estimating site-level GPP (Heinsch et al., 2006).

4.2. A comparison of f_{APAR} techniques

Canopy-level LUE can be considered as an integral of the leaf-level LUE of all leaves (both shaded and sunlit) within the canopy weighted by the strength of the reflected radiation from each leaf to the sensor. Consequently, canopy LUE is influenced by canopy structural characteristics, for example, LAI and the leaf angle distribution. Flux tower observations provide a robust method for the calculation of canopy LUE (Baldocchi, 2008). However, this process requires an independent estimate of f_{APAR} to determine APAR. Three methods were used in this analysis and a comparison is required for use in the operational application of $EVI \times T_m$.

The importance of f_{APAR} is its relationship with vegetation canopy functioning and energy absorption capacity. The first method, measuring PAR at different layers within the canopy, gives direct observations of f_{APAR}. For the other two methods, the calculation of f_{APAR} using in situ LAI measurements is more appropriate from the radiative transfer perspective because LAI is a canopy structural parameter that can be remotely sensed. With available data, calculation of f_{APAR} between in situ LAI (f_{APAR_LAI}) and NDVI (f_{APAR_NDVI}) was compared at the US-MMS site and calculation of f_{APAR} between meteorological PAR (f_{APAR_met}) and NDVI (f_{APAR_NDVI}) was compared at US-WCR.

As shown in Fig. 10, significant correlations are observed both between f_{APAR_NDVI} and f_{APAR_LAI} in US-MMS ($R^2 = 0.63$, $p < 0.001$), and between f_{APAR_NDVI} and f_{APAR_met} in US-WCR ($R^2 = 0.75$, $p < 0.001$). It can be inferred that the main difference among the three methods is the mean values of generated f_{APAR}. Using meteorological PAR measurements appears to give the highest f_{APAR}, followed by the f_{APAR_NDVI} and f_{APAR_LAI}. Therefore, the LUE calculated by the
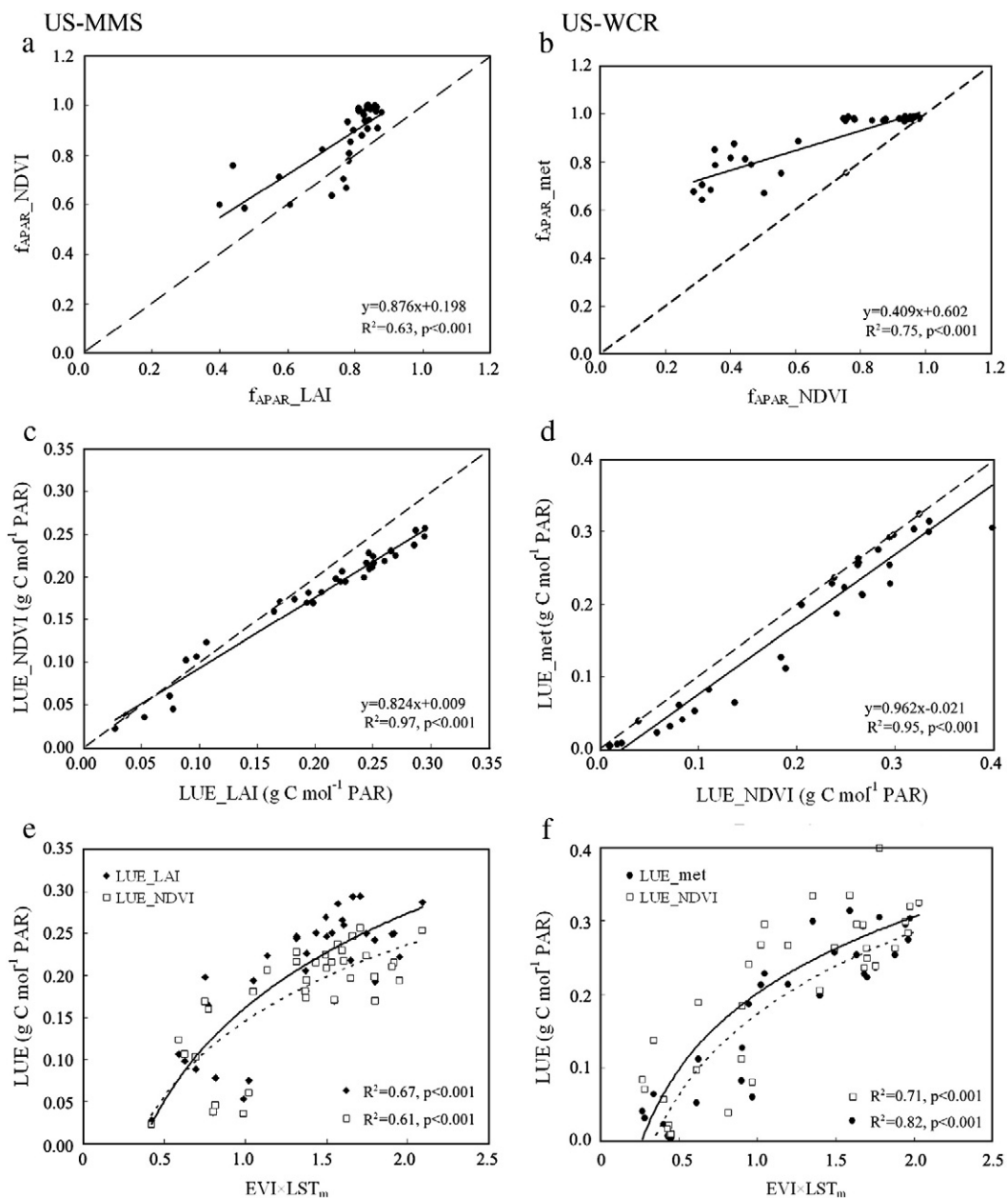

Fig. 10. An analysis of the effect of three f_{APAR} calculation methods on LUE estimation.

three respective methods will fall in an inverted order (Fig. 10c and d). In general, correlations among the three LUEs are very high ($R^2 > 0.95$), indicating that the use of a more general, scalable f_{APAR} calculation method should not affect estimation of variation in LUE substantially. However, attention should be considered in operational applications as differences of 12% and 14% in average LUE are observed between different methods at US-MMS and US-WCR, respectively. The effects are further compared for how coefficients change for our derived algorithm using $EVI \times T_m$ (Fig. 10e and f).

The results first demonstrate that the use of NDVI to estimate f_{APAR} can be a possible method for LUE calculation and this is a reasonable solution due to difficulties in LAI acquisition in forests and unavailability of meteorological PAR profile observations. One issue is that the use of NDVI to calculate f_{APAR} and thus LUE from flux tower GPP could produce an autocorrelation between $EVI \times T_m$ and LUE (i.e., $LUE = GPP/[f(NDVI) \times PAR]$). However, it would be a negative autocorrelation, since an increase in NDVI would increase f_{APAR} and thus decrease LUE, assuming constant GPP and PAR. Secondly, if in situ LAI data or PAR were available, the model $EVI \times T_m$ will give better LUE estimates than the use of NDVI as indicated by the higher coefficients of determination R^2 (0.67 versus 0.61 for US-MMS and 0.82 versus 0.71 for US-WCR). This conclusion also agrees with the above analysis that finds LUE to be dependent on canopy structure, i.e., LAI.

4.3. Limitations of the model

We derived a remote sensing based LUE model using entirely MODIS observations in temperate and boreal forests in North America. However, a number of limitations should be stated in the future application of the algorithm.

First, the model proposed is validated for the estimation of monthly LUE, whereas the feasibility of the model at finer temporal scales is unknown. For example, weekly canopy LUE would be a challenge due to differences in weather conditions. The variability of LUE in such shorter timescales will offer an opportunity to examine the model performance and would be useful to explore the impacts of environmental stresses (e.g., temperature) on the canopy LUE.

We only validated the model in forest landscapes, and its usefulness for other plant functional types (e.g., grassland, woody savannas) needs to be analyzed in future. We suspect the exponential transform of temperature would be more appropriate for ecosystems with higher temperatures. However, the degree of such improvement is still difficult to determine due to the uncertainty of temperature range where it will accelerate or decrease the photosynthesis. Further experimental data are needed to assess the model for high temperate controlled ecosystems.

Theoretical analyses on a more physiologically-based interpretation of the model performances are needed, which would enhance the robustness of model with different ecosystems located at diverse ecoregions. In particular, the model calibration using average EVI and minimum LST for each site lacks a fundamental connection between photosynthesis and its drivers, resulting in unexplained model performances across sites and regions. For example, we found positive correlations between the model performance and the maximum EVI and the average precipitation. However, reasons for such correlations are not well understood as sites with high EVI values are not necessarily experiencing higher precipitations ($R^2 = 0.24$, $p = 0.069$ for all sites, data not shown here). Therefore, it would be a great advantage to explain the model coefficients with physiological or mechanistic terms in future.

5. Conclusions

Light use efficiency is an important variable characterizing plant eco-physiological function and has been widely used to estimate forest productivity from remotely sensed data. By incorporation of both canopy greenness and temperature, here we propose a new algorithm of $EVI \times T_m$ that shows reasonably good estimates of monthly LUE in various forest ecosystems in North America. We also find that a simple metric based on the average of EVI and T_{min} allows for calibration of model coefficients. After calibration, the modeled LUE is shown to reasonably correlate to the flux-measured LUE with an overall RMSE of 0.055 g C mol PAR^{-1} for ten independent sites. The usefulness of the calibrated model is further evaluated in the estimation of GPP and an RMSE of around 37.6 g C m^{-2} month^{-1} has been acquired for all observations, an improvement of 28% over that of the MODIS GPP products, and with an algorithm that does not require additional meteorological inputs.

We have developed a novel model to estimate canopy LUE solely from remote sensing inputs of the form $LUE = (0.21 EVI\_ave + 0.04) \ln(EVI \times \exp(LST/LST_{max})) - 0.04 \ln(LST\_min) + 0.25$. It should be noted that the calibrated model shows a comparable accuracy in LUE estimation between the evergreen and deciduous forests, which is a substantial improvement from models including only EVI. This is especially meaningful for GPP modeling when applied to evergreen species because temporal variability of LUE can be revealed by the seasonal vegetation cycle for deciduous species, while models that can improve estimates in evergreen forests would be of greater importance due to the limited variability in canopy greenness (Garbulsky et al., 2008). The positive impacts of average precipitation quantity on the model performance may imply that other climate variables (e.g., soil water content, vapor pressure deficit) should be integrated to better characterize ecosystem responses to climate change. However, such a process would require more input data at both appropriate spatial and temporal resolutions, requiring a trade-off between the model complexity and accuracy.

References

Amiro, B. D., Barr, A. G., Black, T. A., Iwashita, H., Kljun, N., McCaughey, J. H., Morgenstern, K., Murayama, S., Nesic, Z., Orchansky, A. L., & Saigusa, N. (2006). Carbon, energy and water fluxes at mature and disturbed forest sites, Saskatchewan, Canada. *Agricultural and Forest Meteorology*, *136*, 237–251.

Arain, M. A., Yaun, F., & Black, T. A. (2006). Soil-plant nitrogen cycling modulated carbon exchanges in a western temperate conifer forest in Canada. *Agricultural and Forest Meteorology*, *140*, 171–192.

Baldocchi, D. D. (2008). Breathing of the terrestrial biosphere: Lessons learned from a global network of carbon dioxide flux measurement systems. *Australian Journal of Botany*, *56*, 1–26.

Barr, A. G., Black, T. A., Hogg, E. H., Kljun, N., Morgenstern, K., & Nesic, Z. (2004). Inter-annual variability in the leaf area index of a boreal aspen-hazelnut forest in relation to net ecosystem production. *Agricultural and Forest Meteorology*, *126*, 237–255.

Beer, C., Reichstein, M., Tomelleri, E., Ciais, P., Jung, M., Carvalhais, N., Rödenbeck, C., Arain, M. A., Baldocchi, D., Bonan, G. B., Bondeau, A., Cescatti, A., Lasslop, G., Lindroth, A., Lomas, M., Luyssaert, S., Margolis, H., Oleson, K. W., Roupsard, O., Veenendaal, E., Viovy, N., Williams, C., Ian Woodward, F., & Papale, D. (2010). Terrestrial gross carbon dioxide uptake: Global distribution and covariation with climate. *Science*, *329*, 834–838.

Chen, B., Coops, N. C., Fu, D., Margolis, H. A., Amiro, B. D., Barr, A. G., Black, T. A., Arain, M. A., Bourque, C. P. A., Flanagan, L. B., Lafleur, P. M., McCaughey, J. H., & Wofsy, S. C. (2011). Assessing eddy-covariance flux tower location bias across the Fluxnet-Canada Research Network based on remote sensing and footprint modelling. *Agricultural and Forest Meteorology*, *151*, 87–100.

Chen, J. M., Ju, W. M., Cihlar, J., Price, D., Liu, J., Chen, W. J., Pan, J. J., Black, A., & Barr, A. (2003). Spatial distribution of carbon sources and sinks in Canada's forests. *Tellus, B55*, 622–641.

Cheng, Y. B., Middleton, E. M., Hilker, T., Coops, N. C., Black, T. A., & Krishnan, P. (2009). Dynamics of spectral bio-indicators and their correlations with light use efficiency using directional observations at a Douglas-fir forest. *Measurement Science and Technology, 20*, 1–15.

Cheng, Y. B., Middleton, E. M., Huemmrich, K. F., Zhang, Q., Campbell, P. K. E., Corp, L. A., Russ, A. L., & Kustas, W. P. (2010). Utilizing in situ directional hyperspectral measurements to validate bio-indicator simulations for a corn crop canopy. *Ecological Informatics, 5*, 330–338.

Cook, B. D., Bolstad, P. V., Martin, J. G., Heinsch, F. A., Davis, K. J., Wang, W., Desai, A. R., & Teclaw, R. M. (2008). Using light-use and production efficiency models to predict forest production and carbon exchange during canopy disturbance events. *Ecosystems, 11*, 26–44.

Cook, B. D., Bolstad, P. V., Næsset, E., Anderson, R. S., Garrigues, S., Morisette, J. T., Nickeson, J., & Davis, K. J. (2009). Using LiDAR and quickbird data to model plant production and quantify uncertainties associated with wetland detection and land cover generalizations. *Remote Sensing of Environment, 113*, 2366–2379.

Cook, B. D., Davis, K. J., Wang, W., Desai, A., Berger, B. W., Teclaw, R. M., Martin, J. G., Bolstad, P. V., Bakwin, P. S., Yi, C., & Heilman, W. (2004). Carbon exchange and venting anomalies in an upland deciduous forest in northern Wisconsin, USA. *Agricultural and Forest Meteorology, 126*, 271–295.

Coops, N. C., Hilker, T., Hall, F. G., Nichol, C. J., & Drolet, G. G. (2010). Estimation of light-use efficiency of terrestrial ecosystems from space: A status report. *BioScience, 60*, 788–797.

Coursolle, C., Margolis, H. A., Barr, A. G., Black, T. A., Amiro, B. D., McCaughey, J. H., Flanagan, L. B., Lafleur, P. M., Roulet, N. T., Bourque, C. P. A., Arain, M. A., Wofsy, S. C., Dunn, A., Morgenstern, K., Orchansky, A. L., Bernier, P. Y., Chen, J. M., Kidston, J., Saigusa, N., & Hedstrom, N. (2006). Late-summer carbon fluxes from Canadian forests and peatlands along an east–west continental transect. *Canadian Journal of Forest Research, 36*, 783–800.

Curtis, P. S., Hanson, P. J., Bolstad, P., Barford, C., Randolph, J. C., Schmid, H. P., & Wilson, K. B. (2002). Biometric and eddy-covariance based estimates of annual carbon storage in five eastern North American deciduous forests. *Agricultural and Forest Meteorology, 113*, 3–19.

Denning, A. S., Nicholls, M., Prihodko, L., Baker, I., Vidale, P. L., Davis, K., & Bakwin, P. (2003). Simulated variations in atmospheric CO_2 over a Wisconsin forest using a coupled ecosystem-atmosphere model. *Global Change Biology, 9*, 1241–1250.

Desai, A. R., Bolstad, P. V., Cook, B. D., Davis, K. J., & Carey, E. V. (2005). Comparing net ecosystem exchange of carbon dioxide between an old-growth and mature forest in the upper Midwest, USA. *Agricultural and Forest Meteorology, 128*, 33–55.

Desai, A. R., Richardson, A. D., Moffat, A. M., Kattge, J., Hollinger, D. Y., Barr, A., Falge, E., Noormets, A., Papale, D., Reichstein, M., & Stauch, V. J. (2008). Cross site evaluation of eddy covariance GPP and RE decomposition techniques. *Agricultural and Forest Meteorology, 148*, 821–838.

Dragoni, D., Schmid, H. P., Grimmond, C. S. B., & Loescher, H. W. (2007). Uncertainty of annual net ecosystem productivity estimated using eddy covariance flux measurements. *Journal of Geophysical Research, 112*, D17102, doi:10.1029/2006JD008149.

Drolet, G. G., Huemmrich, K. F., Hall, F. G., Middleton, E. M., Black, T. A., Barr, A. G., & Margolis, H. A. (2005). A MODIS-derived photochemical reflectance index to detect inter-annual variations in the photosynthetic light-use efficiency of a boreal deciduous forest. *Remote Sensing of Environment, 98*, 212–224.

Drolet, G. G., Middleton, E. M., Huemmrich, K. F., Hall, F. G., Amiro, B. D., Barr, A. G., Black, T. A., McCaughey, J. H., & Margolis, H. A. (2008). Regional mapping of gross light-use efficiency using MODIS spectral indices. *Remote Sensing of Environment, 112*, 3064–3078.

Dunn, A. L., Barford, C. C., Wofsy, S. C., Goulden, M. L., & Daube, B. C. (2007). A long-term record of carbon exchange in a boreal black spruce forest: Means, responses to interannual variability, and decadal trends. *Global Change Biology, 13*, 577–590.

Fensholt, R., Sandholt, I., & Rasmussen, M. S. (2004). Evaluation of MODIS LAI, f_{APAR} and the relation between f_{APAR} and NDVI in a semi-arid environment using in situ measurements. *Remote Sensing of Environment, 91*, 490–507.

Filella, I., Porcar-Castell, A., Munne-Bosch, S., Back, J., Garbulsky, M. F., & Peñuelas, J. (2009). PRI assessment of long-term changes in carotenoids/chlorophyll ratio and short-term changes in de-epoxidation of the xanthophyll cycle. *International Journal of Remote Sensing, 30*, 4443–4455.

Gamon, J. A., Serrano, L., & Surfus, J. S. (1997). The photochemical reflectance index: An optical indicator of photosynthesis radiation use efficiency across species, functional types, and nutrient levels. *Oecologia, 112*, 492–501.

Garbulsky, M. F., Peñuelas, J., Gamon, J., Inoue, Y., & Filella, I. (2011). The photochemical reflectance index (PRI) and the remote sensing of leaf, canopy and ecosystem radiation use efficiencies. A review and meta-analysis. *Remote Sensing of Environment, 15*, 281–297.

Garbulsky, M. F., Peñuelas, J., Papale, D., & Filella, I. (2008). Remote estimation of carbon dioxide uptake by a Mediterranean forest. *Global Change Biology, 14*, 2860–2867.

Giasson, M. A., Coursolle, C., & Margolis, H. A. (2006). Ecosystem-level CO_2 fluxes from a boreal cutover in eastern Canada before and after scarification. *Agricultural and Forest Meteorology, 140*, 23–40.

Goerner, A., Reichstein, M., & Rambal, S. (2009). Tracking seasonal drought effects on ecosystem light use efficiency with satellite-based PRI in a Mediterranean forest. *Remote Sensing of Environment, 113*, 1101–1111.

Goetz, S. J., Prince, S. D., & Small, J. (2000). Advances in satellite remote sensing of environmental variables for epidemiological applications. *Advances in Parasitology, 47*, 289–307.

Gu, L., Meyers, T., Pallardy, S. G., Hanson, P. J., Yang, B., Heuer, M., Hosman, K. P., Liu, Q., Riggs, J. S., Sluss, D., & Wullschleger, S. D. (2007). Influences of biomass heat and biochemical energy storages on the land surface fluxes and diurnal temperature range. *Journal of Geophysical Research, 112*, D02107, doi:10.1029/2006JD007425.

Hadley, J. L., Kuzeja, P. S., Daley, M. J., Phillips, N. G., Mulcahy, T., & Singh, S. (2008). Water use and carbon exchange of red oak- and eastern hemlock-dominated forests in the northeastern USA: Implications for ecosystem-level effects of hemlock woolly adelgid. *Tree Physiology, 28*, 615–627.

Hall, F. G., Hilker, T., & Coops, N. C. (2011). PHOTOSYNSAT, photosynthesis from space: Theoretical foundations of a satellite concept and validation from tower and spaceborne data. *Remote Sensing of Environment, 115*, 1918–1925.

Hall, F. G., Hilker, T., Coops, N. C., Lyapustin, A., Huemmrich, K. F., Middleton, E., Margolis, H., Drolet, G., & Black, T. A. (2008). Multi-angle remote sensing of forest light use efficiency by observing PRI variation with shadow fraction. *Remote Sensing of Environment, 112*, 3201–3211.

Heinsch, F., Zhao, M., Running, S., Kimball, J., Nemani, R., Davis, K., Bolstad, P., Cook, B. D., Desai, A. R., Ricciuto, D. M., Law, B. E., Oechel, W. C., Kwon, H., Luo, H., Wofsy, S. C., Dunn, A. L., Munger, J. W., Baldocchi, D. D., Xu, L., Hollinger, D. Y., Richardson, A. D., Stoy, P. C., Siqueira, M. B. S., Monson, R. K., Burns, S. P., & Flanagan, L. B. (2006). Evaluation of remote sensing based terrestrial productivity from MODIS using regional tower eddy flux network observations. *IEEE Transactions on Geoscience and Remote Sensing, 44*, 1908–1925.

Hilker, T., Coops, N. C., Hall, F. G., Black, T. A., Wulder, M. A., Nesic, Z., & Krishnan, P. (2008). Separating physiologically and directionally induced changes in PRI using BRDF models. *Remote Sensing of Environment, 112*, 2777–2788.

Hilker, T., Hall, F. G., Coops, N. C., Lyapustin, A., Wang, Y., Nesic, Z., Grant, N., Black, T. A., Wulder, M. A., Kljun, N., Hopkinson, C., & Chasmer, L. (2010). Remote sensing of photosynthetic light-use efficiency across two forested biomes: Spatial scaling. *Remote Sensing of Environment, 114*, 2863–2874.

Hilker, T., Lyapustin, A., Hall, F. G., Wang, Y., Coops, N. C., Drolet, G., & Black, T. A. (2009). An assessment of photosynthetic light use efficiency from space: Modeling the atmospheric and directional impacts on PRI reflectance. *Remote Sensing of Environment, 113*, 2463–2475.

Hollinger, D. Y., Aber, J., Dail, B., Davidson, E. A., Goltz, S. M., Hughes, H., Leclerc, M., Lee, J. T., Richardson, A. D., Rodrigues, C., Scott, N. A., Varier, D., & Walsh, J. (2004). Spatial and temporal variability in forest-atmosphere CO_2 exchange. *Global Change Biology, 10*, 1689–1706.

Huemmrich, K. F., Gamon, J. A., Tweedie, C. E., Oberbauer, S. F., Kinoshita, G., Houston, S., Kuchy, A., Hollister, R. D., Kwon, H., Mano, M., Harazono, Y., Webber, P. J., & Oechel, W. C. (2010). Remote sensing of tundra gross ecosystem productivity and light use efficiency under varying temperature and moisture conditions. *Remote Sensing of Environment, 114*, 481–489.

Huete, A., Didan, K., Miura, T., Rodriguez, E. P., Gao, X., & Ferreira, L. G. (2002). Overview of the radiometric and biophysical performance of the MODIS vegetation indices. *Remote Sensing of Environment, 83*, 195–213.

Inoue, Y., Peñuelas, J., Miyata, A., & Mano, M. (2008). Normalized difference spectral indices for estimating photosynthetic efficiency and capacity at a canopy scale derived from hyperspectral and CO_2 flux measurements in rice. *Remote Sensing of Environment, 112*, 156–172.

Jenkins, J. P., Richardson, A. D., Braswell, B. H., Ollinger, S. V., Hollinger, D. Y., & Smith, M. L. (2007). Refining light-use efficiency calculations for a deciduous forest canopy using simultaneous tower-based carbon flux and radiometric measurements. *Agricultural and Forest Meteorology, 143*, 64–79.

Monson, R. K., Sparks, J. P., Rosenstiel, T. N., Scott-Denton, L. E., Huxman, T. E., Harley, P. C., Turnipseed, A. A., Burns, S. P., Backlund, B., & Hu, J. (2005). Climatic influences on net ecosystem CO_2 exchange during the transition from wintertime carbon source to springtime carbon sink in a high-elevation, subalpine forest. *Oecologia, 146*, 130–147.

Monteith, J. L. (1972). Solar radiation and production in tropical ecosystems. *Journal of Applied Ecology, 9*, 747–766.

Mu, Q., Zhao, M., & Running, S. W. (2011). Improvements to a MODIS global terrestrial evapotranspiration algorithm. *Remote Sensing of Environment, 115*, 1781–1800.

Nakaji, T., Ide, R., Takagi, K., Kosugi, Y., Ohkubo, S., Nasahara, K. N., Saigusa, N., & Oguma, H. (2008). Utility of spectral vegetation indices for estimation of light conversion efficiency in coniferous forests in Japan. *Agricultural and Forest Meteorology, 148*, 776–787.

Papale, D., & Valentini, A. (2003). A new assessment of European forests carbon exchange by eddy fluxes and artificial neural network spatialization. *Global Change Biology, 9*, 525–535.

Reichstein, M., Falge, E., Baldocchi, D., Papale, D., Aubinet, M., Berbigier, P., Bernhofer, C., Buchmann, N., Gilmanov, T., Granier, A., Grunwald, T., Havrankova, K., Ilvesniemi, H., Janous, D., Knohl, A., Laurila, T., Lohila, A., Loustau, D., Matteucci, G., Meyers, T., Miglietta, F., Ourcival, J. M., Pumpanen, J., Rambal, S., Rotenberg, E., Sanz, M., Tenhunen, J., Seufert, G., Vaccari, F., Vesala, T., Yakir, D., & Valentini, R. (2005). On the separation of net ecosystem exchange into assimilation and ecosystem respiration: Review and improved algorithm. *Global Change Biology, 11*, 1424–1439.

Rouse, J. W., Haas, R. H., Schell, J. A., Deering, D. W., & Harlan, J. C. (1974). Monitoring the vernal advancements and retrogradation of natural vegetation. *NASA/GSFC, Final Report, Greenbelt, MD, USA* (pp. 1–137).

Running, S. W., Nemani, R. R., Heinsch, F. A., Zhao, M., Reeves, M., & Hashimoto, H. (2004). A continuous satellite-derived measure of global terrestrial primary production. *Bioscience, 54*, 547–560.

Schubert, P., Lund, M., Ström, L., & Eklundh, L. (2010). Impact of nutrients on peatland GPP estimations using MODIS time series data. *Remote Sensing of Environment, 114*, 2137–2145.

Schwalm, C. R., Black, T. A., Amiro, B. D., Arain, M. A., Barr, A. G., Bourque, C. P. A., Dunn, A. L., Flanagan, L. B., Giasson, M., Lafleur, P. M., Margolis, H. A., McCaughey, J. H., Orchansky, A. L., & Wofsy, S. C. (2006). Photosynthetic light use efficiency of

three biomes across an east–west continental-scale transect in Canada. *Agricultural and Forest Meteorology*, *140*, 269–286.

Sims, D. A., Rahman, A. F., Cordova, V. D., El-Masri, B. Z., Baldocchi, D. D., Bolstad, P. V., Flanagan, L. B., Goldstein, A. H., Hollinger, D. Y., Misson, L., Monson, R. K., Oechel, W. C., Schmid, H. P., Wofsy, S. C., & Xu, L. (2008). A new model of gross primary productivity of North American ecosystems based solely on the enhanced vegetation index and land surface temperature from MODIS. *Remote Sensing of Environment*, *112*, 1633–1646.

Sims, D. A., Rahman, A. F., Cordova, V. D., El-Masri, B. Z., Baldocchi, D. D., Flanagan, L. B., Goldstein, A. H., Hollinger, D. Y., Misson, L., Monson, R. K., Oechel, W. C., Schmid, H. P., Wofsy, S. C., & Xu, L. (2006). On the use of MODIS EVI to assess gross primary productivity of North American ecosystems. *Journal of Geophysical Research*, *111*, G04015, doi:10.1029/2006JG000162.

Sjöström, M., Ardo, J., Arneth, A., Boulain, N., Cappelaere, B., Eklundh, L., De Grandcourt, A., Kutsch, W. L., Merbold, L., Nouvellon, Y., Scholes, R. J., Schubert, P., Seaquist, J., & Veenendaal, E. M. (2011). Exploring the potential of MODIS EVI for modeling gross primary production across African ecosystems. *Remote sensing of environment*, *115*, 1081–1089.

Tang, J., Bolstad, P. V., Desai, A. R., Martin, J. G., Cook, B. D., Davis, K. J., & Carey, E. V. (2008). Ecosystem respiration and its components in an old-growth forest in the Great Lakes region of the United States. *Agricultural and Forest Meteorology*, *148*, 171–185.

Teklemariam, T., Staebler, R. M., & Barr, A. G. (2009). Eight years of carbon dioxide exchange above a mixed forest at Borden, Ontario. *Agricultural and Forest Meteorology*, *149*, 2040–2053.

Urbanski, S., Barford, C., Wofsy, S., Kucharik, C., Pyle, E., Budney, J., McKain, K., Fitzjarrald, D., Czikowsky, M., & Munger, J. W. (2007). Factors controlling CO_2 exchange on timescales from hourly to decadal at Harvard Forest. *Journal of Geophysical Research*, *112*, G02020, doi:10.1029/2006JG000293.

Viña, A., & Gitelson, A. A. (2005). New developments in the remote estimation of the fraction of absorbed photosynthetically active radiation in crops. *Geophysical Research Letter*, *32*, L17403, doi:10.1029/2005GL023647.

Wan, Z. (2008). New refinements and validation of the MODIS land-surface temperature/-emissivity products. *Remote Sensing of Environment*, *112*, 59–74.

Wu, C., Chen, J. M., & Huang, N. (2011). Predicting gross primary production from the enhanced vegetation index and photosynthetically active radiation: Evaluation and calibration. *Remote Sensing of Environment*, *115*, 3424–3435.

Wu, C., Munger, J. W., Niu, Z., & Kuang, D. (2010). Comparison of multiple models for estimating gross primary production using MODIS and eddy covariance data in Harvard Forest. *Remote Sensing of Environment*, *114*, 2925–2939.

Wu, C., Niu, Z., Tang, Q., Huang, W., Rivard, B., & Feng, J. (2009). Remote estimation of gross primary production in wheat using chlorophyll-related vegetation indices. *Agricultural and Forest Meteorology*, *149*, 1015–1021.

Xiao, X., Zhang, Q., Braswell, B., Urbanski, S., Boles, S., Wofsy, S., Moore, B., III, & Ojima, D. (2004). Modeling gross primary production of temperate deciduous broadleaf forest using satellite images and climate data. *Remote Sensing of Environment*, *91*, 256–270.

Xiao, J., Zhuang, Q., Law, B. E., Chen, J., Baldocchi, D. D., Cook, D. R., Oren, R., Richardson, A. D., Sonia Wharton, S., Ma, S., Martin, T. A., Verma, S. B., Suyker, A. E., Scott, Russell L., Monson, R. L, Litvak, R. K., Hollinger, M., Sun, D. Y., Davis, G., Bolstad, K. J., Burns, P. V., Curtis, S. P., Drake, P. S., Falk, B. G., Fischer, M., Foster, M. L., Gu, D. R., Hadley, L., Katul, J. L., Matamala, G. G., McNulty, R., Meyers, S., Munger, T. P., Noormets, J. W., Oechel, A., Paw U, W. C., Schmid, K. T., Starr, H. P., Torn, G., M. S., & Wofsy, S. C. (2010). A continuous measure of gross primary production for the conterminous United States derived from MODIS and AmeriFlux data. *Remote Sensing of Environment*, *114*, 576–591.

Zhang, Q., Middleton, E. M., Margolis, H. A., Drolet, G. G., Barr, A. G., & Black, T. A. (2009). Can a satellite-derived estimate of the fraction of PAR absorbed by chlorophyll (FAPARchl) improve predictions of light-use efficiency and ecosystem photosynthesis for a boreal aspen forest? *Remote Sensing of Environment*, *113*, 880–888.

Zhao, M., & Running, S. W. (2010). Drought-induced reduction in global terrestrial net primary production from 2000 through 2009. *Science*, *329*, 940–943.

Zhao, M., Running, S. W., & Nemani, R. R. (2006). Sensitivity of Moderate Resolution Imaging Spectroradiometer (MODIS) terrestrial primary production to the accuracy of meteorological reanalyses. *Journal of Geophysical Research*, *111*, G01002, doi: 10.1029/2004JG000004.